Transport of Dendritic Microtubules Establishes Their Nonuniform Polarity Orientation

David J. Sharp, Wenqian Yu, and Peter W. Baas

Department of Anatomy and Program in Neuroscience, The University of Wisconsin Medical School, Madison, Wisconsin 53706

Abstract. The immature processes that give rise to both axons and dendrites contain microtubules (MTs) that are uniformly oriented with their plus-ends distal to the cell body, and this pattern is preserved in the developing axon. In contrast, developing dendrites gradually acquire nonuniform MT polarity orientation due to the addition of a subpopulation of oppositely oriented MTs (Baas, P. W., M. M. Black, and G. A. Banker. 1989. *J. Cell Biol.* 109:3085–3094). In theory, these minus-end-distal MTs could be locally nucleated and assembled within the dendrite itself, or could be transported into the dendrite after their nucleation within the cell body. To distinguish between these possibilities, we exposed cultured hippocampal neurons to nanomolar levels of vinblastine after one of the immature processes had developed into the axon but before the others had become dendrites. At these levels, vinblastine acts as a kinetic stabilizer of MTs, inhibiting further assembly while not substantially depolymerizing existing MTs. This treatment did not abolish dendritic differentiation, which occurred in timely fashion over the next two to three days. The resulting dendrites were flatter and shorter than controls, but were identifiable by their ultrastructure, chemical composition, and thickened tapering morphology. The growth of these dendrites was accompanied by a diminution of MTs from the cell body, indicating a net transfer of MTs from one compartment into the other. During this time, minus-end-distal microtubules arose in the experimental dendrites, indicating that new MT assembly is not required for the acquisition of nonuniform MT polarity orientation in the dendrite. Minus-end-distal microtubules predominated in the more proximal region of experimental dendrites, indicating that most of the MTs at this stage of development are transported into the dendrite with their minus-ends leading. These observations indicate that transport of MTs from the cell body is an essential feature of dendritic development, and that this transport establishes the nonuniform polarity orientation of MTs in the dendrite.

A principal means by which cells establish polarity is via the generation of specialized patterns of microtubule (MT)[1] organization. MTs are cytoskeletal polymers that act both as architectural elements and as substrates for the transport of cytoplasmic constituents. MTs are themselves polar structures, with the plus end favored for assembly over the minus end (Binder et al., 1975; Bergen and Borisy, 1982). This polarity is relevant not only to the assembly properties of the MT, but also to its transport properties. Cytoplasmic organelles interact with molecular motors that translocate specifically toward one end of the MT or the other, and it is in this way that patterns of MT polarity orientation organize the cytoplasm of a cell (for reviews see Brady et al., 1991; Allan et al., 1991). Perhaps the most dramatic example of a cell type in which specialized patterns of MT organization contribute to cell polarity is the neuron. Neurons extend two types of processes, axons and dendrites, that differ from one another in their morphology and subcellular composition. In the axon, MTs are uniformly oriented with their plus ends distal to the cell body, while in the dendrite, MTs are of both orientations (Baas et al., 1988, 1991; Burton, 1988). These distinct MT patterns determine the specific organelles that will translocate from the cell body into each type of process (Baas et al., 1988; Black and Baas, 1989). In addition, the fact that axonal but not dendritic MTs are all oriented with their assembly-favored ends toward the direction of growth may contribute to the fact that axons achieve far greater lengths than dendrites. In these and other ways, the specialized MT arrays of axons and dendrites provide a foundation for critical aspects of neuronal polarity.

In typical nonneuronal cells, a single highly organized MT array is generated via the direct attachment of the minus ends of MTs to a discrete nucleating structure such as

Address all correspondence to P. W. Baas, Department of Anatomy and Program in Neuroscience, The University of Wisconsin Medical School, 1300 University Avenue, Madison, WI 53706. Tel.: (608) 262-7307. Fax: (608) 262-7306.

1. *Abbreviations used in this paper*: AFU, arbitrary fluorescence unit; MAP, microtubule-associated protein; MT, microtubule.

the centrosome (for reviews see Brinkley, 1985; Kellog et al., 1994). In contrast, neurons simultaneously maintain two very different patterns of MT organization, and in neither case are the MTs attached to the centrosome within the cell body of the neuron (Lyser, 1964, 1968; Sharp et al., 1982). Recent studies from our laboratory suggest that the MT array of the axon is elaborated via a combination of MT assembly and transport events (Baas and Joshi, 1992; Baas et al., 1993; Yu et al., 1993, 1994; Ahmad et al., 1994; Yu and Baas, 1994). With regard to polarity orientation, one could envision that either the assembly properties or the transport properties of the MTs account for their uniformly plus-end-distal pattern. In studies aimed at distinguishing between these possibilities, we cultured sympathetic neurons in the presence of nanomolar levels of the anti-MT drug vinblastine (Baas and Ahmad, 1993). At these levels, vinblastine acts as a "kinetic stabilizer" of MTs, inhibiting further assembly while not substantially depolymerizing existing MTs (Jordan and Wilson, 1990; Jordan et al., 1991, 1992; Zheng et al., 1993; Tanaka et al., 1995; for review see Wilson and Jordan, 1994). Thus in the presence of the drug, the only means by which MTs could arise within the axon is by transport from the cell body. Under these conditions, there was a conspicuous transfer of MTs from the cell body into the growing axon, and all of these MTs entered the axon with a plus-end-distal orientation. These results indicate that MTs enter the axon from the cell body specifically with plus-ends leading, and hence, that it is the transport properties of the MTs that establish their characteristic polarity orientation.

Although this scheme is satisfying with regard to the axon, the question remains as to how a very different pattern of MT organization is achieved in the dendrite. Virtually nothing is known about the mechanisms by which the dendritic MT array is elaborated, and in particular whether MT transport plays any role whatsoever. At present, the most useful clue is provided by developmental studies indicating that the plus-end-distal and minus-end-distal MTs in the dendrite arise at different stages in neuronal development (Baas et al., 1989). These studies were performed on cultures of embryonic hippocampal neurons, which undergo a stereotyped sequence of developmental stages (see Dotti et al., 1988). Initially, the neurons extend lamellipodia (stage 1), which coalesce into several essentially similar minor processes (stage 2). One of the minor processes then differentiates into the axon (stage 3), after which those remaining differentiate into dendrites (stage 4). Like the axon, the minor processes contain uniformly plus-end-distal MTs. It is during the transition between stages 3 and 4 that minus-end-distal MTs appear within the developing dendrites.

In the present study, our goals were to determine whether MT transport contributes to the elaboration of the dendritic MT array, and to distinguish between MT transport and MT assembly as the critical factor in the appearance of minus-end-distal MTs during the transition to stage 4. To accomplish this, we utilized the same experimental strategy that proved useful in our previous studies on the axon. At stage 3 of development, after minor processes had formed and one had differentiated into the axon, we experimentally inhibited any further MT assembly by adding to the cultures nanomolar levels of vinblastine. We then determined whether a characteristic dendritic MT array of nonuniform polarity orientation could be established via MT transport alone.

Materials and Methods

Cell Culture

Cultures of embryonic rat hippocampal neurons were prepared as previously described (Goslin and Banker, 1991). Briefly, hippocampi were dissected from 18-d rat embryos, treated with trypsin for 15 min, dissociated with trituration, and plated onto polylysine-treated glass coverslips at a density of ≈1,000 cells/cm^2 in Minimum Essential Medium (Gibco/BRL, Grand Island, NY) containing 10% horse serum. After 4 h of attachment, the coverslips were inverted onto monolayer cultures of astroglial cells growing in plastic culture dishes. At this point, the medium consisted of minimum essential medium, the N2 supplements described by Bottenstein (1985), 1 mM sodium pyruvate, and 0.1% ovalbumin. Cytosine arabinoside was added to the cultures on the third day to a final concentration of 5×10^{-6} M to inhibit the proliferation of nonneuronal cells.

Vinblastine Treatment

Vinblastine sulfate was purchased from Sigma Chemical Company (St. Louis, MO), and dissolved in HPLC grade methanol (Aldrich Chemical Company, Milwaukee, WI) at a concentration of 4 mM. This stock was further diluted with tissue culture medium to a concentration of 0.4 μM, and was added to neuron cultures at a final concentration of 4 nM. Vinblastine was added to the cultures 30 h after plating, when most of the neurons had entered stage 3 of development but before any had entered stage 4. The vinblastine-containing media and the vinblastine stock solutions were prepared fresh for each experiment.

Sample Preparation for Immunofluorescence Microscopy

Cultures were prepared for immunofluorescence microscopy by one method to visualize MTs, and by a different method to visualize microtubule-associated proteins (MAPs). For visualization of MTs, cultures were rinsed in a MT stabilizing buffer termed PHEM (60 mM Pipes, 25 mM Hepes, 10 mM EGTA, 2 mM $MgCl_2$, pH 6.9), and then extracted for 5 min in PHEM supplemented with 10 μm taxol (gift from the National Cancer Institute, Bethesda, MD) and 1% saponin. Cultures were then fixed by the addition of an equal quantity of PHEM containing 8% formaldehyde and 0.25% glutaraldehyde. After 10 min, cultures were rinsed in PBS, postextracted in graded ethanols, and then, to reduce autofluorescence, treated three times 5-min each in 10 mg/ml sodium borohydride in PBS. Cultures were then incubated for 30 min in a blocking solution containing 2% bovine serum albumen and 5% normal goat serum in PBS, incubated overnight at 4°C with primary antibody diluted in PBS, rinsed three times for 5-min each with PBS, incubated again with blocking solution for 30 min, incubated for 1 h at 37°C with a fluorescent second antibody, rinsed four times 5-min each with PBS, and mounted in a medium containing 90% glycerol, 100 mg/ml DABCO, and 1 mg/ml *p*-phenylenediamine, and 10% PBS. The primary antibody, used at 1:500, was a mouse monoclonal purchased from Amersham Corp. (Arlington Heights, IL) that recognizes all forms of β-tubulin. The second antibody, used at 1:100, was a Cy-3–conjugated goat anti-mouse purchased from Jackson ImmunoResearch (West Grove, PA). For visualization of MAPs, cultures were rinsed in PBS, fixed for 10 min in PBS containing 4% formaldehyde and 0.1% glutaraldehyde, rinsed twice in PBS, postextracted in graded ethanols, rinsed twice in PBS, then treated with sodium borohydride, blocking solutions, and antibodies as indicated above. Cultures were double-labeled with a mouse monoclonal antibody against the adult form of MAP-2 (used at 1:500) and a rabbit polyclonal antibody against tau (used at 1:100), both of which were provided to us by Dr. Itzhak Fischer. The second antibodies, both used at 1:100, were a lissamine rhodamine–conjugated goat anti–mouse and a fluorescein-conjugated goat anti–rabbit, both purchased from Jackson ImmunoResearch and both pre-absorbed for minimal cross-reactivity. All primary antibody incubations were for 18 h at 4°C, and all second antibody incubations were for 1 h at 37°C.

Immunofluorescence Analyses

Cultures prepared for immunofluorescence microscopy were visualized and images were captured using the Zeiss LSM 410 Laser Confocal Microscope (Carl Zeiss Incorporated, Thornwood, NY). Images were obtained using the Zeiss 63× Plan-APOCHROMAT objective, and the pinhole on the confocal system was opened maximally so that most or all of the width of each neuronal processes was captured in a single image. For samples stained to visualize MTs, images were captured in two ways. First, to compare MT levels among different cells, the same brightness and contrast settings were used throughout, and standard black-and-white images were captured. All optical sections comprising the neurons were reconstructed into a single image using the Zeiss software. Fluorescence intensities were then quantified using NIH-Image software (provided free of charge from the National Institutes of Health, Bethesda, MD). Because the LSM 410 is equipped with photomultiplier tubes that are linear with regard to their detection of fluorescence intensities, differences in fluorescence intensities accurately reflect differences in MT mass (provided that antibody treatments and levels of photobleach are kept similar among samples). Fluorescence intensities were calculated separately for each compartment of the cell (cell body, minor processes, dendrites, and axon), expressed in arbitrary fluorescence units (AFUs), and the mean values ($n = 6$) were coalesced into a stacked bar graph. Statistical analyses were performed using the Students t test. Second, to better visualize the differences in the levels of MTs in different regions of individual cells, we used a function of the Zeiss software termed glow-scale pseudocolor. This function maintains high resolution while expressing fluorescence intensity in a pseudocolor scale in which white is the highest, red is the lowest, and shades of yellow and orange represent intermediate levels of intensity. For these analyses, brightness and contrast were optimized separately for each cell to provide information on differences in the distribution of MTs within each cell. For samples stained to visualize MAPs, the same brightness and contrast settings were used throughout, and the lissamine-rhodamine and fluorescein images were combined, using NIH-Image, into a single figure in which MAP-2 is shown in red, tau is shown in blue, and overlapping regions are shown in shades of purple.

Electron Microscopy

In preparation for electron microscopy, the neuron cultures were fixed at 37°C in 0.1 M cacodylate containing 2% glutaraldehyde, and processed as previously described (Yu and Baas, 1994; modified from Banker and Goslin, 1991). Briefly, after 20 min of fixation, the cultures were rinsed twice for 5-min each in 0.1 M cacodylate, postfixed for 5 min in 1% OsO_4, rinsed twice for 2 min in NaCl, rinsed twice for 2 min in water, contrasted for 30 min in 5% aqueous uranyl acetate, dehydrated in ethanols, and embedded in LX-112 (Ladd Research Industries, Burlington, VT). After curing overnight at 60°C, the glass coverslips were dissolved from the resin by a 10-min treatment with hydrofluoric acid. For enhancement of their light microscopic appearance, embedded cultures were stained at 60°C for 30 min with 1% toluidine blue. Cells of interest were circled with a diamond marker objective and their images were recorded using a Sony videoprinter. Thin sections with a uniform thickness of 100 nm were obtained with an Ultracut S Ultramicrotome (Reichert-Jung, Vienna, Austria), picked-up on formvar-coated slot grids, stained with uranyl acetate and lead citrate, and observed with a CX100 electron microscope (JEOL USA, Inc., Peabody, MA).

Microtubule Polarity Analyses

To determine the polarity orientation of the MTs in developing dendrites, we used our modification (Baas et al., 1987, 1989) of the standard protocol (Heidemann and McIntosh, 1980; for review see Heidemann, 1991). In this procedure, cultures are lysed in the presence of a special MT assembly buffer containing exogenous brain tubulin, and then prepared for electron microscopy. The exogenous tubulin adds onto existing MTs in the form of lateral protofilament sheets that appear as "hooks" on the MTs when viewed in cross section. The curvature of the hook reveals the polarity orientation of the MT; a clockwise hook indicates that the plus end of the MT is directed toward the observer, while a counterclockwise hook indicates the opposite. In the present study, cultures were rinsed twice in PBS (to remove tissue culture medium and residual vinblastine that might interfere with hook formation), and then treated for 2 min at 37°C with 0.06% Brij 58 in a MT assembly buffer (0.5 M Pipes, 0.1 mM EGTA, 0.01 mM EDTA, 0.1 mM $MgCl_2$, 2.5% DMSO, 0.5 mM GTP) containing 1.2 mg/ml MT protein. This mixture was then replaced with an identical mixture lacking the Brij 58 detergent, and cultures were incubated for 28 additional minutes at 37°C. The cultures were then fixed by the addition of an equal quantity of 4% glutaraldehyde, and prepared for electron microscopy. Cross-sections of the dendrites were taken, and hooks were interpreted and scored as previously described (Heidemann and McIntosh, 1980; Heidemann, 1991). Hooks were judged to be clockwise or counterclockwise from the vantage point of the distal tip of the dendrites.

Results

Dendritic Differentiation in the Presence of Vinblastine

The goal of these studies was to determine the role, if any, of MT transport in the elaboration and organization of the dendritic MT array. Our strategy was to pharmacologically arrest MT assembly prior to dendritic differentiation, and then analyze the features of a dendritic array generated via MT transport alone. As described in the Materials and Methods section, this was accomplished by introducing 4 nM vinblastine into cultures of embryonic hippocampal neurons at stage 3 of development. Fig. 1 *A* shows a typical stage 3 neuron (30 h in culture) with several minor processes, one of which has differentiated into the axon. Fig. 1 *B* shows a typical stage 4 neuron (96 h in culture). The axon has elongated and the remaining minor processes have developed into thick tapering dendrites. Fig. 1 *C* shows an experimental stage 4 neuron (96 h in culture; vinblastine added at 30 h). The minor processes have developed into thick tapering processes that were somewhat shorter and flatter but otherwise similar to control dendrites. Interestingly, the axon was generally shorter than at stage 3, although axon length was difficult to discern in many cases due to overlap and/or fasciculation with the axons of neighboring cells. These characteristics were displayed by ≈75% of the neurons in the culture. The remaining cells did not develop thick tapering processes, and died by the third day in culture. The cells that formed the thickened processes began to deteriorate and died by the sixth day in culture, but were typically robust through the fourth and fifth days. For this reason, analyses were performed on 4-d cultures.

To determine whether the thick tapering processes that developed in the presence of vinblastine were indeed dendrites, we analyzed two defining features of dendritic composition, their complement of MAPs and their organelle composition. With regard to the former, we focused on the adult form of MAP-2, a protein that becomes progressively concentrated in developing dendrites and is progressively vacated from the minor process that develops into the axon (Caceres et al., 1984). For immunofluorescence analyses, cultures were double labeled with a monoclonal antibody against adult MAP-2 and a polyclonal antibody against tau, a MAP that is present throughout the neuron at all stages of development (Caceres et al., 1986; Dotti et al., 1987). During stage 3, adult MAP-2 was concentrated in the cell body and the proximal regions of the minor processes and axon (Fig. 1 *D*). In control stage 4 cells, adult MAP-2 was concentrated in the cell bodies and dendrites (Fig. 1 *E*). Similarly, in experimental stage 4 cells, tau appeared throughout the neuron while adult MAP-2 was concentrated in cell bodies and the thick tapering processes (Fig. 1 *F*). With regard to organelle composition,

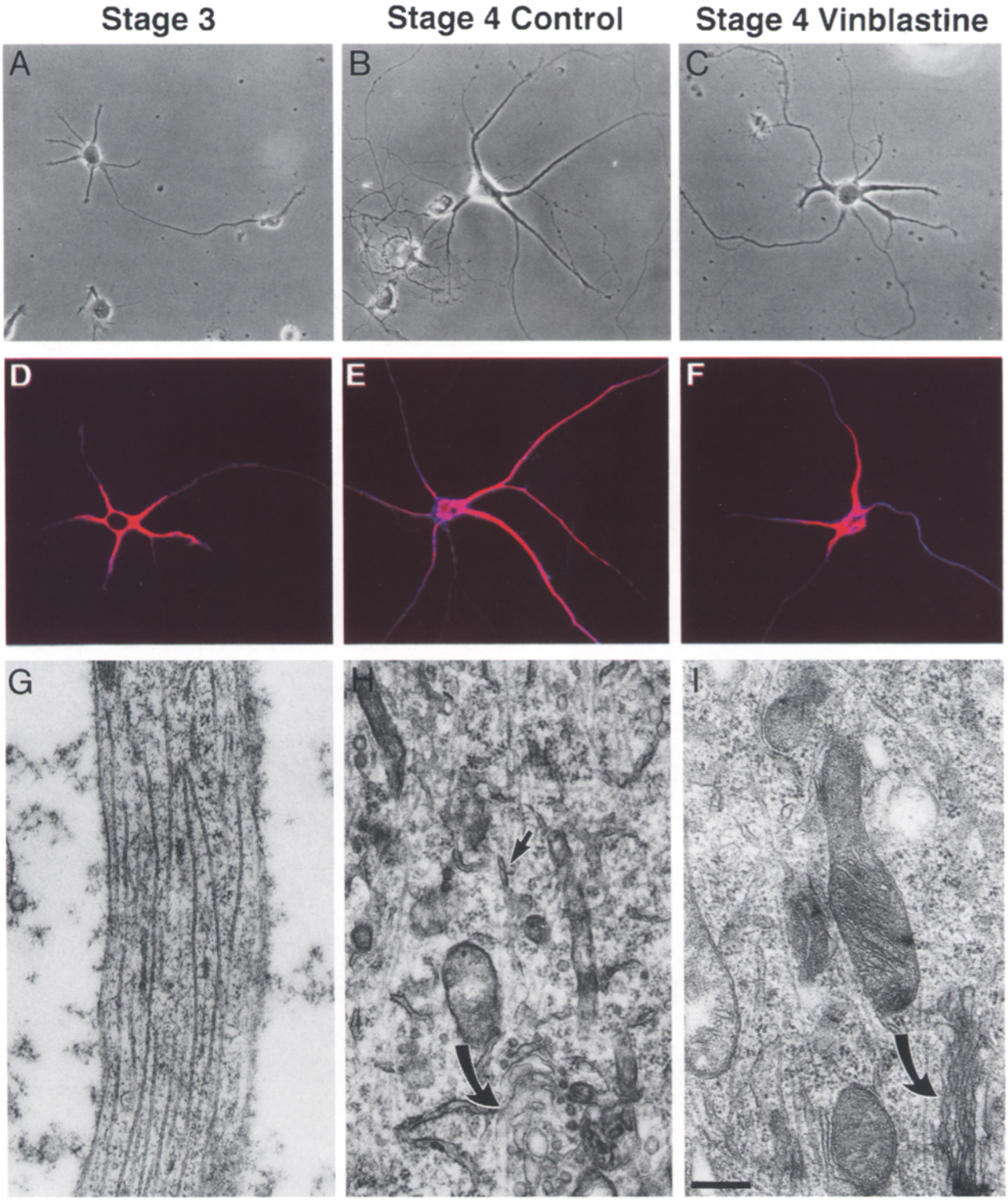

Figure 1. Dendritic differentiation in the presence of vinblastine. (*A–C*) Phase-contrast micrographs of neurons at stage 3 (30 h in culture), stage 4 (96 h in culture), and experimental stage 4 (96 hours in culture; 4 nM vinblastine added at 30 h), respectively. The stage 3 cell shows multiple minor processes and one axon. At stage 4, the minor processes have developed into multiple thick tapering dendrites. In the experimental cells, the minor processes have developed into thick tapering processes that are shorter and flatter but otherwise similar to control dendrites. Axons are distinguishable in both control and experimental stage 4 cells by their thin non-tapering morphology. (*D–F*) Double-label immunofluorescence images of stage 3, control stage 4, and experimental stage 4 cells, respectively. Tau is shown in blue, adult MAP-2 is shown in red, and their overlap is shown in purple. The adult form of MAP-2 was selected for these studies because it is a better marker for developing dendrites than total MAP-2 staining. In all cases, high levels of tau appear throughout the neuron. Adult MAP-2 staining is also present throughout the neurons at earlier stages of development, but progressively vacates the axon as it develops. In stage 3 cells, adult MAP-2 is concentrated in the cell body and more proximal regions of the minor processes and axon. In control stage 4 cells, adult MAP-2 is concentrated in the cell body and dendritic processes. In experimental stage 4 cells,

dendrites are distinguished from axons by the presence in dendrites of Golgi elements and a dense population of ribosomes (see Black and Baas, 1989). The minor processes of stage 3 cells contained some ribosomes (markedly fewer than in dendrites; see Deitch and Banker, 1993), but no Golgi elements (Fig. 1 *G*). Golgi elements were generally dispersed in the dendrites of control stage 4 cells and did not appear in stacks, and hence were difficult to identify with confidence in electron micrographs. However, with some effort and analysis of serial sections, we located discernible Golgi stacks in the proximal regions of control dendrites and trails of vesicular elements that appeared to break off from the stacks and invade the middle region of the dendrite (Fig. 1 *H*). In the thickened processes extended by experimental stage 4 cells, Golgi stacks were clearly identifiable throughout the length of the processes (Fig. 1 *I*). (We suspect that Golgi elements were less dispersed in these processes because of lower levels of the MTs along which they translocate.) In addition, the thick tapering processes of the experimental cells contained similar numbers of ribosomes as the control dendrites, severalfold the numbers found in the minor processes of stage 3 cells. These results indicate that minor processes differentiated into dendrites (defined by morphological and compositional criteria) in the presence of 4 nM vinblastine. Hereafter, we will refer to these processes as "experimental dendrites."

Effects of Vinblastine on Microtubule Levels in the Neuron

Before focusing on MT organization in the experimental dendrites, it was first necessary for us to confirm that the vinblastine treatment had the desired effect on MT levels. If vinblastine inhibited MT assembly as expected, the total MT levels in experimental stage 4 cells should not exceed the total levels in stage 3 cells. To test this, we used quantitative immunofluorescence microscopy to determine the total MT mass within stage 3 cells, control stage 4 cells, and experimental stage 4 cells. For this, cultures were extracted in a MT-stabilizing buffer to remove free tubulin, fixed, and stained with a general β-tubulin antibody. Fluorescence intensities were measured and expressed in AFUs as described in Materials and Methods. Stage 3, control stage 4, and experimental stage 4 cells contained 274,000 ± 91,300, 525,000 ± 148,000, and 215,000 ± 95,800 AFUs of MT mass, respectively. These data indicate that control cells underwent a nearly twofold increase in MT mass during the transition from stage 3 to stage 4 ($P < 0.005$). The mean MT mass in experimental stage 4 cells was ≈20% lower than that for the stage 3 cells, suggesting that the vinblastine treatment may actually have induced net MT disassembly. This result is favorable for our purposes because net MT disassembly provides extra confidence that any MT assembly that might have occurred was minimal. However, it should be noted that statistical analyses ($P < 0.2$) suggest a reasonable possibility that there may not be a significant difference between stage 3 and control stage 4 cells. In either case, the results are consistent with our goals, indicating that the vinblastine treatment curtailed MT assembly and may or may not have induced some MT disassembly.

Changes in Microtubule Distribution during the Transition to Stage 4

To investigate the movements that MTs undergo during the transition from stage 3 to 4, we analyzed the distribution of MTs within the cells. In a first set of studies, the levels of MT mass were quantified separately for the cell body, minor processes, dendrites, and axons of each cell. The data (mean ± standard deviation) are shown in Table I and are coalesced into a stacked bar graph shown in Fig. 2. At stage 3, the cell body contained 43,300 ± 35,400 AFUs of MT polymer. (We suspect that the rather high standard deviation relates to an ongoing accumulation of MT polymer that occurs within the cell body during stage 3, and that this accumulation is essential for the transition into stage 4. Additional studies are underway to test this hypothesis.) The minor processes contained 88,700 ± 29,400 and the axon contained 142,000 ± 29,400 AFUs of polymer. In control stage 4 neurons, after most of the minor processes differentiated into dendrites, the MT levels were roughly twofold higher in each compartment. In experimental stage 4 neurons, the MT mass in the cell body was roughly half that in the cell body at stage 3 ($P < 0.10$), indicating that MTs had moved out of the cell body and into the processes. Consistent with this conclusion, the dendrites that formed in the presence of vinblastine contained over 33% more MT polymer than the minor processes in stage 3 ($P < 0.0025$), indicating a transfer of polymer from the cell body into developing dendrites. (These same experimental dendrites contained ≈32% less polymer than control dendrites at stage 4 [$P < 0.0025$].) Interestingly, the MT mass in the experimental axon decreased by over 50% compared to the stage 3 axon ($P < 0.001$), suggesting a net transfer of MTs from the axon back to the cell body. (This finding is consistent with the morphological observation that axons often become shorter in experimental stage 4 neurons.) Taken together, these data indicate that there is a net transfer of MT from the cell body into developing dendrites during the transition

adult MAP-2 is concentrated in the cell body and the thick tapering processes. (*G–I*) Transmission electron micrographs of a minor process from a stage 3 cell, a dendrite from a control stage 4 cell, and a thick tapering process from an experimental stage 4 cell, respectively. In the minor processes, a small number of ribosomes but no discernible Golgi elements are present, and MTs are apparent. Control dendrites contain somewhat sparser and less paraxial MTs, significantly more ribosomes, and large numbers of internal membranous elements not found in minor processes or axons (*h, arrows*). We suspect that many of these are Golgi elements in that they can be seen dispersing from what appear to be fragmenting stacks of Golgi in more proximal regions of the dendrite (*curved arrow*). The thick tapering processes of the experimental cells contain lower amounts of MT polymer, but like the control dendrites are rich in ribosomes and Golgi (*I, curved arrow*). Golgi elements are easier to discern in experimental processes, with unmistakable stacks appearing even far down their lengths. These results indicate that dendrites (defined by morphological, compositional, and ultrastructural criteria) differentiate in the presence of vinblastine. Bar: (*A, B, D, E, G,* and *H*) 20 μm and (*C, F,* and *I*) 0.5 μm.

Table I. Effects of Vinblastine on Microtubule Levels in the Neuron

Cell stage / MT mass (AFU)	Stage 3 control	Stage 4 control	Stage 4 vinblastine
Total cell	274,000 ± 91,300	525,000 ± 148,000	215,000 ± 95,800
Cell body	43,300 ± 35,400	84,500 ± 36,800	20,100 ± 11,900
Minor processes	88,700 ± 29,400	20,700 ± 13,800	15,900 ± 17,900
Dendrites	–	142,000 ± 18,900	97,200 ± 24,400
Axon	142,000 ± 29,400	277,000 ± 43,900	62,300 ± 36,900

from stage 3 to 4. In addition, the transport of MTs into dendrites occurs at the expense of the cell body and takes priority over the axon during this critical phase of neuronal development.

Additional information relevant to MT transport derives from higher resolution analyses on the distribution of MTs within individual neurons. For these analyses, fluorescence images were expressed in glow-scale pseudocolor, in which white indicates highest intensity, red indicates the least, and shades of orange and yellow indicate intermediate levels (see Materials and Methods). Surprisingly useful insights were obtained from analyses on the controls neurons alone. Fig. 3 *A* shows a cell in stage 3, while Fig. 3 (*B–D*) show cells in stage 4. At stage 3, the highest levels of polymer appeared in the minor processes and the proximal region of the axon. At stage 4, the highest levels of polymer appeared in the developing dendrites. All cells contained high levels of polymer within discrete regions of the cell body (yellow and/or white) that were continuous with high levels of polymer within some of the processes. In many of the cells (see especially Fig. 3 *B*), the polymer within these processes could be traced to a single discrete point in the cell body, presumably their site of origin.

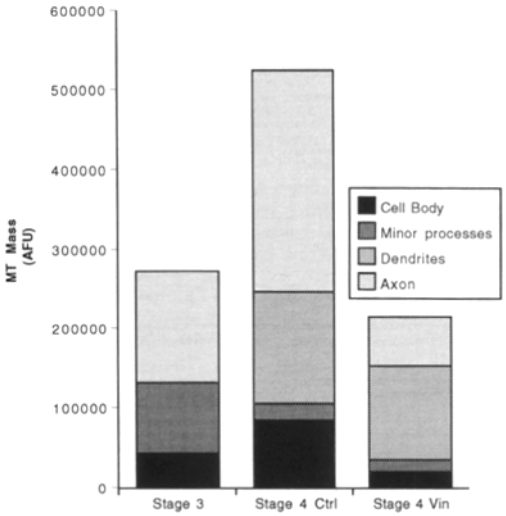

Figure 2. Effects of vinblastine on microtubule levels in the neuron. MT levels within stage 3 neurons, control stage 4 neurons, and experimental stage 4 neurons were quantified using immunofluorescence microscopy (see Materials and Methods). MT levels were quantified separately in the cell body, minor processes, axon, and dendrites, and expressed in arbitrary fluorescence units (*AFU*). Data are shown as a stacked bar graph ($n = 6$ for each condition; see Table I for standard deviations). Five main conclusions can be drawn from the data. First, the total MT mass increased by nearly twofold in each neuronal compartment during the normal transition from stage 3 to 4. Second, the total MT mass in experimental stage 4 neurons was essentially the same or lower than the total MT mass in stage 3 neurons. Third, in the presence of vinblastine, MT mass in the cell body decreased by over half compared to the cell body at stage 3. Fourth, the dendrites that developed in the presence of vinblastine contained over 33% more MT polymer than the minor processes in stage 3, but contained ≈32% less polymer than control dendrites. Fifth, the MT mass in the vinblastine-axon decreased by over 50% compared to the stage 3 axon. More detailed analyses and statistics are provided in the Results section.

Fig. 3 (*E–H*) show experimental stage 4 neurons. In all of these neurons, the fluorescence intensity was markedly diminished in the cell body (see especially Fig. 3 *H*). The experimental dendrites contained the highest levels of MTs (which appeared as a fairly continuous white and yellow band), but unlike the situation in control neurons, the MT staining was not continuous with staining in the cell body. In the neuron shown in Fig. 3 *E*, the white and yellow band appeared to break up in the proximal few microns of the dendrites, and only low levels of yellow staining appeared in the cell body. The other neurons showed only red staining in the cell body. In the neuron shown in Fig. 3 *F*, the cell body and proximal dendrites contained relatively low levels of polymer (and hence were red in color), and the white and yellow band began in the more medial region of the dendrite, several microns from the cell body. Figs. 3 (*G* and *H*) show cells with multiple dendrites, each varying with regard to the position of the white and yellow band of MTs. In the neuron shown in Fig. 3 *H*, the cell body was virtually devoid of MTs, which appeared only as a small cluster of red fragments. Results entirely similar to these were obtained in electron microscopic analyses (data not shown). Collectively, these higher resolution analyses provide strong visual support for the transport of MTs into developing dendrites, and show that even when MT assembly is inhibited, existing MTs continue their proximodistal march down these processes.

Polarity Orientation of Microtubules Transported into the Dendrite

Having established a paradigm for studying the transport of MTs into the dendrite, we next wished to determine whether it is the transport properties of the MTs that establish their characteristic nonuniform polarity orientation. We previously established that MTs in the minor processes and axon are uniformly plus-end-distal, and during the transition into stage 4, the developing dendrites acquire a subpopulation of minus-end-distal MTs (Baas et al., 1989; see Introduction). To determine whether the MTs transported into the dendrite during this transition are of the opposite orientation, we used the standard MT polarity determination protocol to assess MT polarity orientation in the dendrites of experimental stage 4 neurons. As described in Materials and Methods, cells were extracted in a special buffer in the presence of exogenous brain tubulin. Under these conditions, the exogenous tubulin adds onto existing MTs in the form of lateral ap-

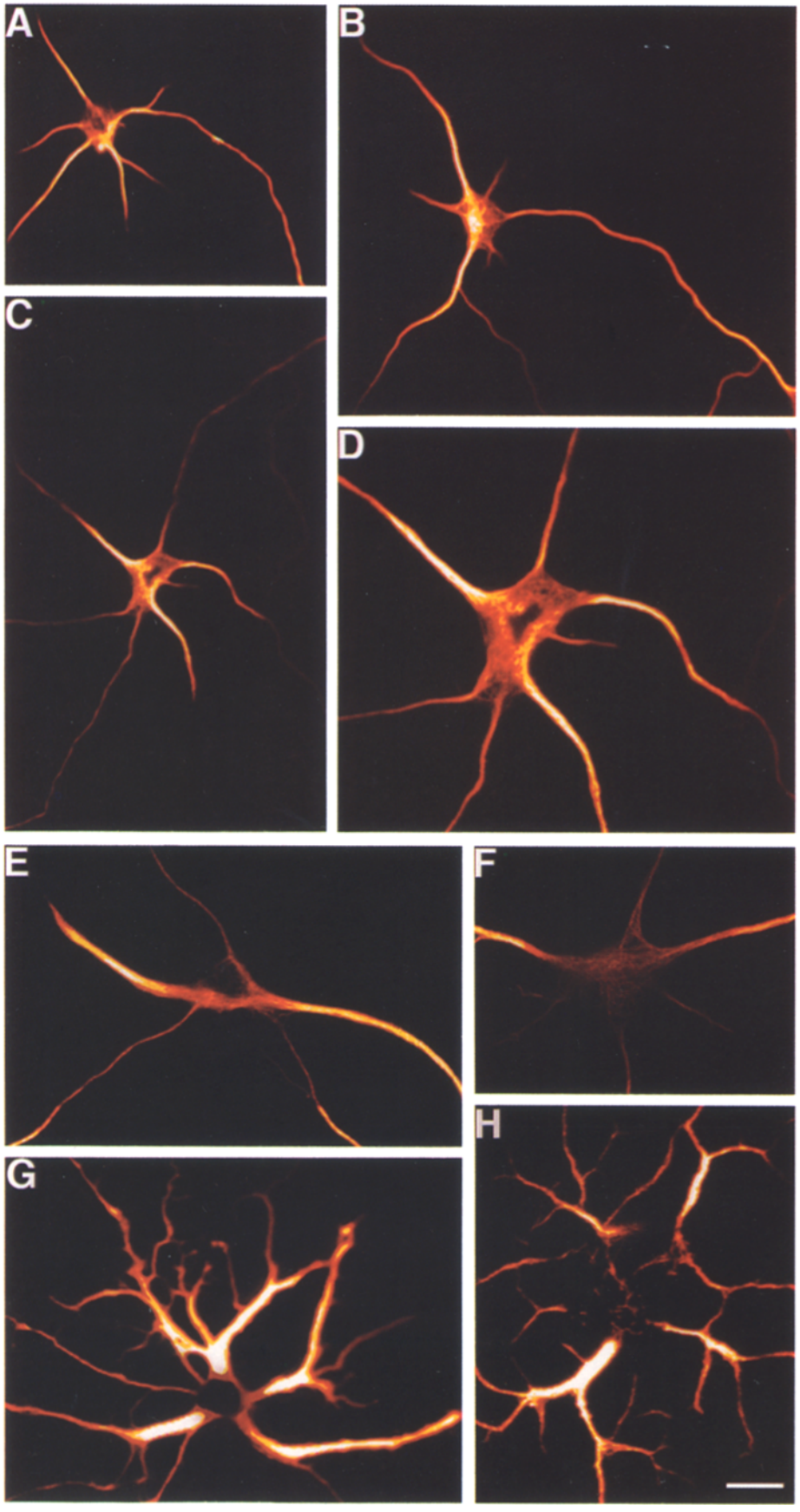

Figure 3. Distribution of microtubules in control and experimental neurons. Neurons were prepared for immunofluorescence visualization of MTs and images were obtained as described in Materials and Methods. Images are shown in glow-scale pseudocolor, in which white indicates highest intensity, red indicates the least, and shades of orange and yellow indicate intermediate levels. Intensities (color patterns) are optimized to show distribution of polymer within an individual cell. *A* shows a control cell in late stage 3, while *B* and *C* show control cells in stage 4. All cells contain high levels of MTs within discrete regions of the cell body (yellow or white). These regions are continuous with high levels of polymer within some of the processes. At late stage 3, highest levels of polymer appear in the minor processes and the proximal region of the axon. At stage 4, the highest levels of polymer appear in the developing dendrites. *D* is a higher magnification view of a region of the cell shown in *C*. *E–H* shows experimental stage 4 neurons (96 h in culture; vinblastine added at 30 h) at progressive phases of dendritic development. In all of the experimental neurons, the fluorescence intensity is markedly diminished in the cell body compared to the developing dendrites. The neuron in *H* shows only a small number of MT fragments remaining in the cell body. The dendrites contain the highest levels of MT polymer, but unlike the situation in control neurons, the MT staining is not continuous with staining in the cell body. In many cases (see especially *F*), the highest levels of MT staining appear at some point beyond (distal to) the proximal region of the dendrites. Bar: (*A–C*, and *E–H*), 20 μm, (*D*), 9 μm.

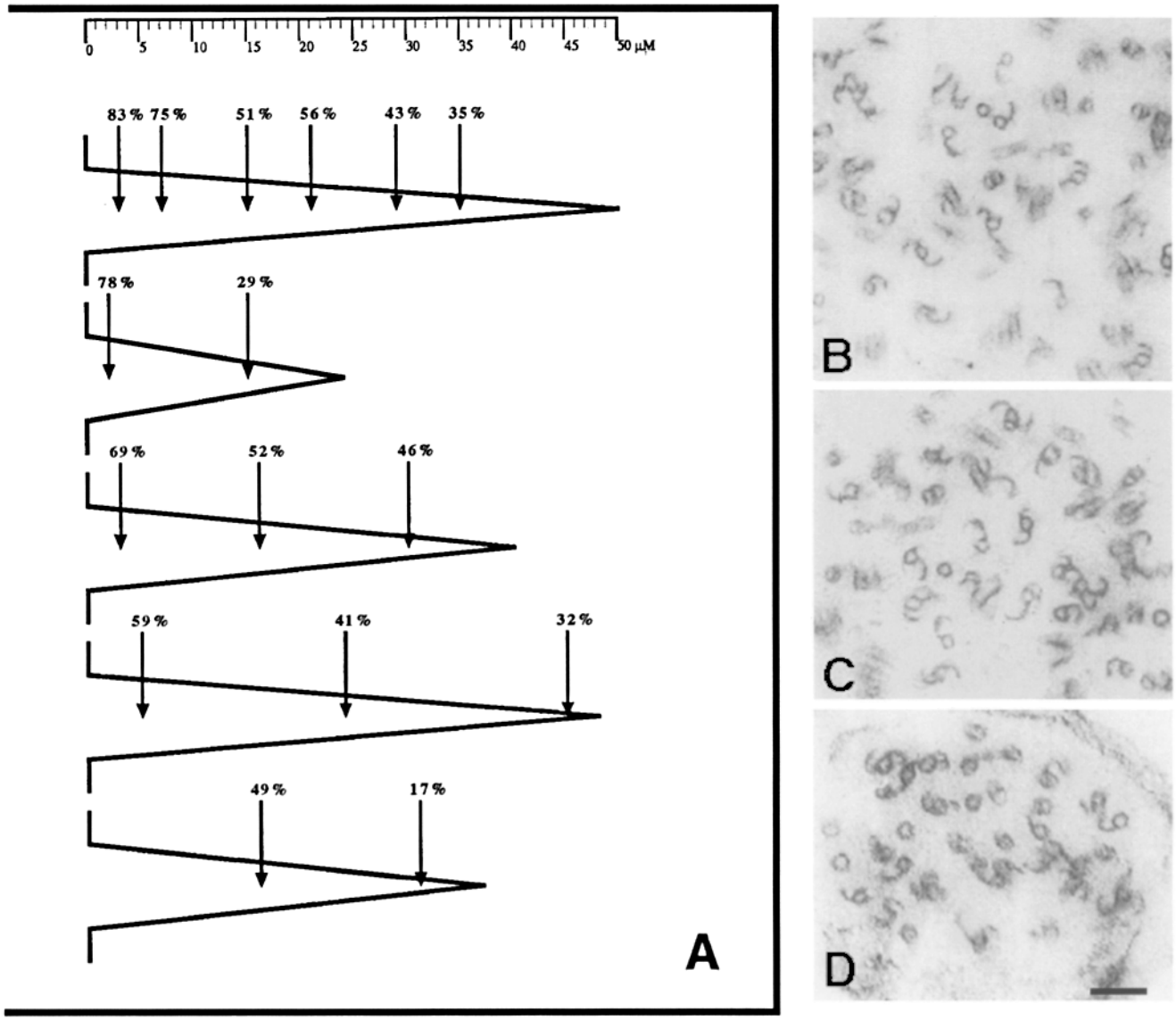

Figure 4. Microtubule polarity analyses. The standard method was used to assess MT polarity orientation in experimental dendrites (see Materials and Methods and Results). As viewed from the distal tips of the processes, clockwise hooks indicate plus-end-distal MTs, while counterclockwise hooks indicate minus-end-distal MTs. Shown in *A* are schematics of the five different experimental dendrites analyzed, each of which was analyzed at multiple points along its length. The proportion of counterclockwise hooks (minus-end-distal MTs) is indicated at each sampling sites, and sample electron micrographs of a proximal region and a midregion of an experimental dendrite are shown in *B* and *C*, respectively. The proximal regions of the processes contained predominantly minus-end-distal MTs, the distal regions contained predominantly plus-end-distal MTs, and the middle regions contained roughly equal proportions of the two. *D* shows an axon from an experimental stage 4 neuron, with uniformly plus-end-distal MTs (predominantly clockwise hooks). Bar, 0.1 μm.

pendages that appear as hooks when viewed in cross-section. All analyses were interpreted from the perspective of the distal tips of the dendrites, such that clockwise and counterclockwise hooks indicate plus-end-distal and minus-end-distal MTs, respectively. As expected, control axons contained uniformly plus-end-distal MTs, and control dendrites contained roughly equal numbers of plus-end-distal and minus-end-distal MTs in their midregions (data not shown; see Baas et al., 1988, 1989). The axons of experimental stage 4 neurons contained uniformly plus-end-distal MTs (see Fig. 4 *D*).

Five experimental dendrites were analyzed at multiple sites along their length. Because the MTs in these dendrites were not perfectly parallel to one another, over half the microtubules were sectioned at a skewed angle and were uninterpretable. Therefore, we scored interpretable hooks in 5–15 consecutive thin sections for each data point along the dendrites length. For each of these positions, 50–500 MTs were scored and summed, and the data were expressed in terms of the percentage of counterclockwise hooks (minus-end-distal MTs) at each position. Each of the five experimental dendrites showed a proximodistal decrease in the proportion of minus-end-distal MTs (see Fig. 4 *A*). Similar to the situation in control dendrites, the midregions of the experimental dendrites contained roughly equal proportions of MTs of each orientation (Fig.

4 *C*). However unlike the situation in controls, the microtubules in the proximal region of the dendrites, those microtubules most recently transported into the dendrite from the cell body, were predominantly minus-end-distal (Fig. 4 *B*). These results indicate that minus-end-distal MTs arise in dendrites even in the absence of new MT assembly, and hence that it is the transport properties of dendritic MTs that establish their nonuniform polarity orientation. The fact that the proximal regions of the experimental dendrites contained predominantly minus-end-distal MTs indicates that during the transition from stage 3 to 4, MTs are transported into developing dendrites predominantly or exclusively with minus-ends leading.

Discussion

There is great interest in elucidating the mechanisms by which axonal MTs achieve their uniform polarity orientation and dendritic MTs achieve their nonuniform polarity orientation. In theory, these distinct patterns of polarity orientation could arise from the assembly properties of the MTs or from their transport properties. An effective strategy for dissecting the contribution of MT transport from that of assembly is to culture cells in the presence of nanomolar levels of vinblastine. At these low levels, vinblastine acts as a kinetic stabilizer of MTs, inhibiting new assembly without substantially depolymerizing existing MTs. Thus any changes in the distribution of MTs that occur in the presence of the drug can be attributed to the translocation of MTs from one location in the cell to another. Previously we reported that axons grown under these conditions acquire uniformly plus-end-distal MTs in similar fashion to control axons, indicating that the transport properties of axonal MTs are sufficient to establish their characteristic polarity orientation (Baas and Ahmad, 1993). In the present study, we sought to determine whether MT transport also contributes to the elaboration of the dendritic array, and if so whether the transport properties of dendritic MTs establish their very different pattern of polarity orientation. To accomplish this, nanomolar levels of vinblastine were added to cultured hippocampal neurons at stage 3 of development, after one of the minor processes had developed into the axon but before the others had developed into dendrites.

Dendritic differentiation was not inhibited by the lack of new MT assembly within the neuron. However, even though there was no net increase in total MT levels in the neuron, the conversion of a minor process into a dendrite was accompanied by a clear increase in MT levels within these processes. This increase was offset by a concomitant diminution of MTs from the cell body, indicating a net transfer of MTs from one compartment of the neuron into the other. As the dendrites developed, there were additional indications of MT movements. In control neurons, the MT array of the dendrite was continuous with high concentrations of MTs in the cell body, while in experimental neurons, the MTs in the dendrite became disjointed from the MTs in the cell body and appeared at progressively greater distances down the length of the dendrites. These observations indicate that MTs are transported from the cell body into the dendrite, and that once inside the dendrite, these MTs continue to translocate in a proximodistal direction. Unlike the minor processes, which contain only plus-end-distal MTs, the dendrites that differentiated in the presence of vinblastine contained both plus-end-distal and minus-end-distal MTs. In fact, the MTs in the more proximal regions of the experimental dendrites, those most recently transported in from the cell body, were predominantly minus-end-distal, indicating that most or all of the MTs that translocated into these processes did so with their minus-ends-leading. Collectively, these results indicate that MT transport is an essential element in the elaboration of the dendritic MT array, and that it is the transport properties of dendritic MTs that establish their nonuniform polarity orientation.

Mechanisms for Elaborating the Dendritic Microtubule Array

Progress has been slow in elucidating the mechanisms by which the dendritic MT array is elaborated, in large part because most attention has been focused on the MT array of the axon. In our earlier work on the dendrite, we suggested that the nonuniform polarity orientation of dendritic MTs may result from the local nucleation and assembly of minus-end-distal MTs within the dendrite itself (Baas et al., 1988, 1989). If this were correct, it would only be necessary for the neuron to transport MTs with plus-ends leading. However, we subsequently found that γ-tubulin, a protein required for MT nucleation in living cells, is absent from the dendrite, and present only at the centrosome within the cell body of the neuron (Baas and Joshi, 1992). This observation suggested that all MTs destined for dendrites, like those destined for axons, are probably nucleated at the centrosome, released, and then actively transported into these processes. Although provocative, this idea was initially unsettling because it called for a more sophisticated MT transport machinery than previously imagined. However, the present results are entirely consistent with this conclusion, indicating a fundamental role for MT transport in the generation of nonuniform MT polarity orientation in the dendrite. In addition, support for a centrosomal origin for dendritic MTs is provided by our observations on control neurons, showing that the high levels of MTs within developing dendrites can often be traced back to a single discrete point in the cell body of the neuron.

The mechanism by which axonal and dendritic MTs are transported remains speculative. At present, the best information on MT-based transport derives from studies on organelle transport along MTs and from in vitro work (for reviews see Allan et al., 1991; Brady, 1991). These studies have established that MT-based transport events require a molecular motor that interacts with both the MT and with another cytoplasmic component (the "substrate"). Either the substrate or the MT will translocate in response to the motor. One class of motors, the kinesins, moves organelles toward the plus end of the MT, while another class of motors, the dyneins, moves organelles toward the minus end of the MT. Given that motion is relative, the kinesins will move a MT against a stationary substrate with minus-end-leading, while dyneins will move a MT with plus-end-leading. Whether these or as yet undiscovered motors are responsible for the transport of MTs into axons and/or

dendrites is unknown. Also unknown is the substrate against which the MTs translocate. One possibility is that MTs slide relative to one another, with different MTs rendered stationary at different moments in time (see Lasek, 1988; Baas and Ahmad, 1993). If this is correct, one could envision that axonal MTs translocate against MTs of the same polarity orientation, while dendritic MTs translocate against MTs of the opposite orientation. Precedent exists for the former in the case of MT sliding during ciliary movements (Summers and Gibbons, 1971), and for the latter with regard to MT sliding in the mitotic spindle (for review see McIntosh, 1994). Perhaps the most challenging question concerns how an individual MT in the cell body associates with the proper machinery to translocate into either the axon or a dendrite. Clearly, additional studies will be required to elucidate the specific motors and the substrates involved in the transport of axonal and dendritic MTs, and our experimental paradigm may prove useful for these future efforts.

We suspect that a complex cascade of biochemical events regulates MT transport in developing neurons. For example, it is possible that different molecular motors are expressed or activated at different stages of development (see for example Sekine et al., 1994). Compelling in this regard is our observation (both on control and experimental neurons) that MTs are transported preferentially over the axon into developing dendrites during the transition from stage 3 to 4. Another possibility is that differences in the composition of the MTs may regulate their interactions with different transport motors. For example, MTs richer in MAP-2 may interact with motors differently than MTs richer in tau. Support for this possibility derives from in vitro work showing that high levels of MAP-2 can inhibit the interaction of MTs with certain transport motors more effectively than high levels of tau (Lopez and Sheetz, 1993). With regard to the MAPs, it should be noted that expression of tau or MAP-2 in nonneuronal cells induces the formation of MT bundles, but different MAPs do not result in differences in the polarity orientation of MTs within these bundles (Baas et al., 1991; Chen et al., 1992; LeClerc et al., 1993). However, these nonneuronal cells do not have the same transport machinery as neurons, and hence the possibility remains that MAPs might help regulate the transport motors responsible for the patterns of MT polarity orientation in axons and dendrites. Future efforts will focus on the factors that regulate MT transport, and how these factors are coordinated during critical phases of neuronal development.

Concluding Remarks

The generation of highly organized MT arrays is essential for the development of cell polarity. Each MT within a cell has its own intrinsic polarity, and organizing the MTs with regard to their polarity profoundly affects the architecture and cytoplasmic organization of the cell. Traditionally, cell biologists have focused on the attachment of MTs to discrete nucleating structures such as centrosomes or basal bodies as a means of organizing MTs. However, many cell types, particularly those that become polar, maintain MT arrays that are not attached to a singular nucleating structure and yet the MTs within these arrays are highly organized with regard to their polarity. Neurons are a particularly good example in that they simultaneously maintain two very different but highly organized MT arrays, one for the axon and another for the dendrites, neither of which is attached to the centrosome. While the MTs that find their way into axons and dendrites apparently originate at the centrosome, these MTs must be re-organized after they are released into the cytoplasm. In the present study and in our previous work on the axon, we have shown that the complex MT arrays of axons and dendrites are organized by the transport properties of the MTs that comprise these arrays. Thus, at least in neuronal cells, MT transport represents another key strategy that cells have for organizing their microtubules. We suspect that MT transport is highly specialized in the neuron, and in fact, quintessential for defining the neuronal phenotype. However, it seems likely that other cell types may also utilize transport as a strategy for organizing MTs that become detached from their nucleation sites. Additional studies on MT transport both in neurons and nonneuronal cells will be of great interest in this regard.

We thank Dr. John White of The University of Wisconsin for helpful discussions on quantitative fluorescence microscopy, and Dr. Itzhak Fischer of The Medical College of Pennsylvania for kindly providing antibodies against tau and MAP-2.

This work was supported by National Institutes of Health grant NS 28785 and National Science Foundation grant IBN-9209939 to P. W. Baas, who is also the recipient of a Research Career Development Award from the National Institutes of Health. D. J. Sharp is supported by National Institutes of Health grant GM 07507 to the Neuroscience Training Program at The University of Wisconsin.

Received for publication 15 February 1995 and in revised form 28 March 1995.

References

Ahmad, F. J., H. C. Joshi, V. E. Centonze, and P. W. Baas. 1994. Inhibition of microtubule nucleation at the neuronal centrosome compromises axon growth. *Neuron.* 12:271–280.

Allan, V. J., R. D. Vale, and F. Navone. 1991. Microtubule-based organelle transport in neurons. *In* The Neuronal Cytoskeleton. R. D. Burgoyne, editor. Wiley-Liss, New York. 257–282.

Baas, P. W., and F. J. Ahmad. 1993. The transport properties of axonal microtubules establish their polarity orientation. *J. Cell Biol.* 120:1427–1437.

Baas, P. W., and H. C. Joshi. 1992. γ-tubulin distribution in the neuron: implications for the origins of neuritic microtubules. *J. Cell Biol.* 119:171–178.

Baas, P. W., L. A. White, and S. R. Heidemann. 1987. Microtubule polarity reversal accompanies regrowth of amputated neurites. *Proc. Natl. Acad. Sci. USA.* 84:5272–5276.

Baas, P. W., J. S. Deitch, M. M. Black, and G. A. Banker. 1988. Polarity orientation of microtubules in hippocampal neurons: uniformity in the axon and nonuniformity in the dendrite. *Proc. Natl. Acad. Sci. USA.* 85:8335–8339.

Baas, P. W., M. M. Black, and G. A. Banker. 1989. Changes in microtubule polarity orientation during the development of hippocampal neurons in culture. *J. Cell Biol.* 109:3085–3094.

Baas, P. W., T. P. Pienkowski, and K. S. Kosik. 1991. Processes induced by tau expression in Sf9 cells have an axon-like microtubule organization. *J. Cell Biol.* 115:1333–1344.

Baas, P. W., F. J. Ahmad, T. P. Pienkowski, A. Brown, and M. M. Black. 1993. Sites of microtubule stabilization for the axon. *J. Neurosci.* 13:2177–2185.

Banker, G., and K. Goslin. 1991. Characterizing and studying neuronal cultures. *In* Culturing Nerve Cells. G. Banker and K. Goslin, editors. MIT Press, Cambridge, MA. 75–109.

Bergen, L., and G. G. Borisy. 1980. Head-to-tail polymerization of microtubules in vivo. Electron microscope analysis of seeded assembly. *J. Cell Biol.* 84:141–150.

Binder, L. I., W. Dentler, and J. L. Rosenbaum. 1975. Assembly of chick brain tubulin onto flagellar microtubules from *Chalamydomonas* and sea urchin sperm. *Proc. Natl. Acad. Sci. USA.* 72:1122–1126.

Black, M. M., and P. W. Baas. 1989. The basis of polarity in neuron. *Trends Neurosci.* 12:211–214.

Bottenstein, J. 1985. Growth and differentiation of neural cells in defined me-

dia. *In* Cell Culture in the Neurosciences. J. E. Bottenstein and G. Sato, editors. Plenum Press, New York. 3–44.
Brady, S. T. 1991. Molecular motors in the nervous system. *Neuron.* 7:521–533.
Brinkley, B. R. 1985. Microtubule organizing centers. *Annu. Rev. Cell Biol.* 1:145–172.
Burton, P. R. 1988. Dendrites of mitral cell neurons contain microtubules of opposite polarity. *Brain Res.* 473:107–115.
Caceres, A., G. Banker, O. Steward, L. Binder, and M. Payne. 1984. MAP2 is localized to the dendrites of hippocampal neurons which develop in culture. *Dev. Brain Res.* 13:314–318.
Caceres, A., G. A. Banker, and L. Binder. 1986. Immunocytochemical localization of tubulin and microtubule-associated protein 2 during the development of hippocampal neurons in culture. *J. Neurosci.* 6:714–722.
Chen, J., Y. Kanai, N. J. Cowan, and N. Hirokawa. 1992. Projection domains of MAP-2 and tau determine spacings between microtubules in dendrites and axons. *Nature (Lond.).* 360:674–677.
Deitch, J. S., and G. A. Banker. 1993. An electron microscopic analysis of hippocampal neurons in culture: Early stages in the emergence of polarity. *J. Neurosci.* 13:4301–4315.
Dotti, C. G., G. A. Banker, and L. I. Binder. 1987. The expression and distribution of the microtubule-associated proteins tau and microtubule-associated protein 2 in hippocampal neurons in the rat brain in situ and in cell culture. *Neuroscience.* 23:212–130.
Dotti, C. G., C. A. Sullivan, G. A. Banker. 1988. The establishment of polarity by hippocampal neurons in culture. *J. Neurosci.* 8:1454–1468.
Goslin, K., and G. Banker. 1991. Rat hippocampal neurons in low-density culture. *In* Culturing Nerve Cells. G. Banker and K. Goslin, editors. MIT Press, Cambridge, MA. 251–281.
Heidemann, S. R. 1991. Microtubule polarity determination based on formation of protofilament hooks. *Methods Enzymol.* 196:517–519.
Heidemann, S. R., and J. R. McIntosh. 1980. Visualization of the structural polarity of microtubules. *Nature (Lond.)* 286:517–519.
Heidemann, S. R., J. M. Landers, and M. A. Hamborg. 1981. Polarity orientation of axonal microtubules. *J. Cell Biol.* 91:661–665.
Jordan, M. A., and L. Wilson. 1990. Kinetic analysis of tubulin exchange at microtubule ends at low vinblastine concentrations. *Biochemistry.* 29:2730–2739.
Jordan, M. A., D. Thrower, and L. Wilson. 1991. Mechanism of inhibition of cell proliferation by vinca alkaloids. *Cancer Res.* 51:2212–2222.
Jordan, M. A., D. Thrower, and L. Wilson. 1992. Effects of vinblastine, podophyllotoxin and nocodazole on mitotic spindles: implications for the role of microtubule dynamics in mitosis. *J. Cell Sci.* 102:402–416.
Joshi, H. C., and P. W. Baas. 1993. A new perspective on microtubules and axon growth. *J. Cell Biol.* 121:1191–1196.
Kellog, D. R., M. Moritz, and B. M. Alberts. 1994. The centrosome and cellular organization. *Annu. Rev. Biochem.* 63:639–674.
Lasek, R. J. 1988. Studying the intrinsic determinants of neuronal form and function. *In* Intrinsic Determinants of Neuronal Form and Function. R. J. Lasek and M. M. Black, editors. Alan R. Liss, New York. 1–58.
LeClerc, N., K. S. Kosik, N. Cowan, T. P. Pienkowski, and P. W. Baas. 1993. Process formation in Sf9 cells induced by the expression of a microtubule-associated protein 2c-like construct. *Proc. Natl. Acad. Sci. USA.* 90:6223–6227.
Lopez, L. A., and M. P. Sheetz. 1993. Steric inhibition of cytoplasmic dynein and kinesin motility by MAP-2. *Cell Motil. & Cytoskeleton.* 24:1–16.
Lyser, 1964. Early differentiation of motor neuroblasts in the chick embryo as studied by electron microscopy. I. General aspects. *Dev. Biol.* 10:433–466.
Lyser, K. M. 1968. An electron microscopic study of centrioles of differentiating neuroblasts. *J. Embryol. Exp. Morphol.* 20:343–354.
McIntosh, J. R. 1994. The roles of microtubules in chromosome movement. *In* Microtubules. J. S. Hyams and C. W. Lloyd, editors. Wiley-Liss, New York. 413–434.
Sekine, Y., Y. Okada, Y. Noda, S. Kondo, H. Aizawa, R. Takemura, and N. Hirokawa. 1994. A novel microtubule-based motor protein (KIF4) for organelle transports, whose expression is regulated developmentally. *J. Cell Biol.* 127:187–201.
Sharp, G. A., K. Weber, and M. Osborn. 1982. Centriole number and process formation in established neuroblastoma cells and primary dorsal root ganglion neurons. *Eur. J. Cell Biol.* 29:97–103.
Summers, K., and I. R. Gibbons. 1971. Adenosine triphosphate-induced sliding of tubules in trypsin treated flagella of sea urchin sperm. *Proc. Natl. Acad. Sci. USA.* 68:3092–3096.
Tanaka, E., T. Ho, and M. W. Kirschner. 1995. The role of microtubule dynamics in growth cone motility and axonal growth. *J. Cell Biol.* 128:139–155.
Wilson, L., and M. A. Jordan. 1994. Pharmacological probes of microtubule function. *In* Microtubules. J. S. Hyams and C. W. Lloyd, editors. 59–83.
Yu, W., and P. W. Baas. 1994. Changes in microtubule number and length during axon differentiation. *J. Neurosci.* 14:2818–2829.
Yu, W., V. E. Centonze, F. J. Ahmad, and P. W. Baas. 1993. Microtubule nucleation and release from the neuronal centrosome. *J. Cell Biol.* 122:349–359.
Zheng, J., R. E. Buxbaum, and S. R. Heidemann. 1993. Investigation of microtubule assembly and organization accompanying tension-induced neurite initiation. *J. Cell Sci* 104:1239–1250.